Molecular Therapy
Oncolytics
Original Article

AMERICAN SOCIETY of GENE & CELL THERAPY

Targeting Histone Methyltransferase DOT1L by a Novel Psammaplin A Analog Inhibits Growth and Metastasis of Triple-Negative Breast Cancer

Woong Sub Byun,[1] Won Kyung Kim,[1] Hae Ju Han,[2] Hwa-Jin Chung,[1] Kyungkuk Jang,[2] Han Sun Kim,[1] Sunghwa Kim,[1] Donghwa Kim,[1] Eun Seo Bae,[1] Sunghyouk Park,[1] Jeeyeon Lee,[2] Hyeung-geun Park,[2] and Sang Kook Lee[1]

[1]College of Pharmacy, Natural Products Research Institute, Seoul National University, Seoul 08826, Republic of Korea; [2]College of Pharmacy, Research Institute of Pharmaceutical Sciences, Seoul National University, Seoul 08826, Republic of Korea

Triple-negative breast cancer (TNBC) is the most intractable cancer in women with a high risk of metastasis. While hypermethylation of histone H3 catalyzed by disruptor of telomeric silencing 1-like (DOT1L), a specific methyltransferase for histone H3 at lysine residue 79 (H3K79), is reported as a potential target for TNBCs, early developed nucleoside-type DOT1L inhibitors are not sufficient for effective inhibition of growth and metastasis of TNBC cells. We found that TNBC cells had a high expression level of DOT1L and a low expression level of E-cadherin compared to normal breast epithelial cells and non-TNBC cells. Here, a novel psammaplin A analog (PsA-3091) exhibited a potent inhibitory effect of DOT1L-mediated H3K79 methylation. Consistently, PsA-3091 also significantly inhibited the proliferation, migration, and invasion of TNBC cells along with the augmented expression of E-cadherin and the suppression of N-cadherin, ZEB1, and vimentin expression. In an orthotopic mouse model, PsA-3091 effectively inhibited lung metastasis and tumor growth by the regulation of DOT1L activity and EMT biomarkers. Together, we report here a new template of DOT1L inhibitor and suggest that targeting DOT1L-mediated H3K79 methylation by a novel PsA analog may be a promising strategy for the treatment of metastatic breast cancer patients.

INTRODUCTION

Breast cancer (BC) is the second leading cause of cancer death for women worldwide. Among BCs, approximately 15% to 20% are classified as triple-negative breast cancers (TNBCs), which do not express estrogen, progesterone, and HER2 receptors.[1,2] TNBCs are considered to be the most aggressive cancers, as they do not respond to endocrine therapies or other targeted therapies, and they have a high risk of recurrence. Previous studies have revealed that breast cancer cells frequently metastasize to the lung, bone, and brain tissues through lymphatic vessels, and 90% of deaths caused by breast cancer are associated with metastasis.[3–5] Recent studies reported that breast cancer metastasis is partly governed by epigenetic process.[6,7] In particular, histone methyltransferases (HMTs), such as disruptor of Telomeric silencing 1-like (DOT1L) or G9a, regulates the expression of E-cadherin, a major cell-junction molecule, in breast cancer cells.[8–10] Loss of E-cadherin is the most typical process in tumor metastasis.[8] Therefore, targeting epigenetic processes in metastatic breast cancers are urgently required to decrease the rate of breast cancer metastasis and to further increase the survival rate for patients with metastatic BCs.

It is known that DOT1L, a HMT, utilizes *S*-adenosylmethionine (SAM) as a methyl donor to regulate the methylation of histone H3 at lysine residue 79 (H3K79), and it plays an important role in the regulation of transcription, cell cycle, and DNA damage response.[11–14] Recent studies have shown that the DOT1L expression level is crucial for tumor development, especially in leukemia with mixed-lineage leukemia (MLL) fusion proteins, and participates in the activation of leukemic transcription, suggesting an oncogenic role of DOT1L in leukemia. Therefore, DOT1L has been considered a potential therapeutic target for *MLL*-rearranged leukemia.[15–17] However, only a few studies on the association between DOT1L and breast cancers have been reported.

Zhang et al.[18] have reported that the pharmacologic inhibition of H3K79 methylation suppresses the self-renewal of breast cancer stem cells (BCSCs), breast cancer proliferation, migration, and invasion. However, the detailed mechanisms of the oncogenic potential and clinical relevance of DOT1L in solid tumors, including breast cancer, have not yet been clearly elucidated. Recently, Cho et al.[8] suggested that the cooperation of DOT1L with c-Myc-p300 is important for the regulation of both the epithelial-mesenchymal transition (EMT) and CSC properties in breast cancer through the epigenetic activation of EMT-transcription factors (TFs), providing a novel mechanism of epigenetic regulation of DOT1L-mediated

Received 24 June 2019; accepted 19 September 2019;
https://doi.org/10.1016/j.omto.2019.09.005.

Correspondence: Sang Kook Lee, College of Pharmacy, Natural Products Research Institute, Seoul National University, 1 Gwanak-gu, Gwanak-ro, Seoul 08826, Republic of Korea.
E-mail: sklee61@snu.ac.kr

Table 1. DOT1L Inhibitory Activity of the Psammaplin A Analogs

Psammaplin A Analogs (1 μM)	DOT1L Inhibition (%)
PsA-1011	36.6 ± 1.9
PsA-3051	35.5 ± 2.3
PsA-3052	33.1 ± 2.3
PsA-3054	34.2 ± 2.2
PsA-3091	43.9 ± 1.8
PsA-3092	39.8 ± 1.1
PsA-3041	38.9 ± 1.9
PsA-1016	33.6 ± 2.6
PsA-3271	34.5 ± 2.4
PsA-1018	36.5 ± 1.8
EPZ-5676 (100 nM)	75.5 ± 3.0

The data are expressed as the mean (± SD) of three independent experiments, each performed in triplicate, and are presented relative to control. EPZ-5676 was used as a positive control.

transcription of EMT enhancers. Moreover, the expression of DOT1L was highly related with lymph node metastasis in ovarian cancer.[19] Although the possible role of DOT1L in the metastasis of solid tumors has been suggested, early developed nucleoside-containing inhibitors of DOT1L, such as EPZ-5676, did not show effective suppression of tumor growth and metastasis of solid tumor cells, including breast cancer cells.[20] Therefore, the procurement of new template compounds for the regulation of DOT1L activity for solid cancers, including aggressive metastatic TNBCs, is required to improve the survival rate of cancer patients.

An attractive strategy toward this goal is to develop compounds that selectively inhibit the binding of the cofactor SAM with specific protein methyltransferases. DOT1L catalyzes an S_N2 reaction of the H3K79 ε-NH2 of the substrate nucleosome with the methyl group of SAM.[21] Therefore, compounds that selectively interact with DOT1L and competitively block the binding with SAM could inhibit H3K79 methylation.

In our continuing efforts to provide better insights into the role of DOT1L regulation in breast cancer and the development of epigenetic inhibitors for metastatic breast cancer therapy, we evaluated the effects of psammaplin A (PsA) analogs on the activity of DOT1L. PsA, a natural marine product isolated from the *Psammaplysilla* sponge, has been previously reported to be an antitumor agent that functions as an effective regulator of epigenetic enzymes, including histone deacetylases (HDACs) and DNA methyltransferases (DNMTs).[22,23] Although PsA showed a promising pharmacological activity against cancer cells, two major drawbacks were evoked with the low abundance of natural sources and poor pharmacokinetic properties. In particular, the pharmacokinetic study with an intravenous injection in mice revealed the short half-life and rapid systemic clearance,[24] suggesting the needs of the improvement of the pharmacokinetic property with PsA. Therefore, we rationally designed and synthesized the PsA analogs and primarily evaluated the biological activity with the inhibition of cancer cell growth and histone deacetylase activity.[25] Based on the findings, in this study, we further extended to evaluate the biological activity of PsA analogs against DOT1L, one of the major histone-modifying enzymes associated with cancer cell metastasis and proliferation. Herein, the antitumor and anti-metastatic activities of PsA analogs were explored through modulation of the DOT1L-mediated EMT process in human aggressive and metastatic breast cancer cells.

RESULTS

The Effects of Psammaplin A Analogs on DOT1L Activity and Proliferation of Human Cancer Cells

To explore potent small-molecule inhibitors of DOT1L, 116 novel analogs of PsA were evaluated with DOT1L cell-free enzyme activity assay. Among these compounds, some analogs (PsA-1011, -3051, -3052, -3054, -3091, -3092, -3041, -1016, -3271, and -1018) exhibited a greater than 30% inhibition rate against DOT1L activity at the test concentration of 1 μM (Table 1). From these results, PsA-3091, a heteromonomeric structural analog, showed the most potent inhibitory activity, with an IC_{50} value of 1.77 μM (Figures 1A and 1B). Since some PsA analogs exhibited inhibitory activity toward DOT1L in the cell-free biochemical assay, we further evaluated the inhibitory effects of compounds on DOT1L activity in cancer cells by western blot analysis using an antibody against di-methylated lysine 79 residues of histone H3 (H3K79me2), the biological target of DOT1L.[26] Consistent with the result obtained for cell-free DOT1L inhibitory activity, the overexpressed level of H3K79 methylation (H3K79me2) in MDA-MB-231 breast cancer cells was most significantly suppressed by PsA-3091 (Figure 1C). Therefore, further analysis was performed with PsA-3091 to elucidate the detailed mechanism of action in cancer cell proliferation and anti-metastatic activities in aggressive triple-negative breast cancer cells.

PsA-3091 Suppresses DOT1L Activity via the Interacting Binding Pocket of the Enzyme

To understand the binding interactions between PsA-3091 ligand and DOT1L, molecular docking studies were carried out using the X-ray crystal structure of DOT1L (PDB: 3SR4). DOT1L has a deep binding pocket for the cofactor SAM. As shown in Figure 1D, PsA-3091 fits snugly into the deep and narrow binding pocket of DOT1L, suggesting a tight binding to DOT1L. The *t*-butyl phenyl group of the ligand has hydrophobic interactions with Phe223 and Pro133, which were identified as critical residues for the interaction with the adenosine moiety of SAM.[27] The OH of the oxime has a hydrogen bond with the carbonyl oxygen of Glu134, whereas the NH of the adjacent amide group forms hydrogen bonds with two oxygen atoms of the carboxylate side chain of Glu186 (Figures 1E and 1F). These hydrogen bonds constitute a tight network involving Lys187, Glu186, Gly163, and Glu134, which contributes to the specific recognition of PsA-3091 by these residues in the binding pocket. These data suggest that PsA-3091 might interfere with the interaction between DOT1L and SAM.

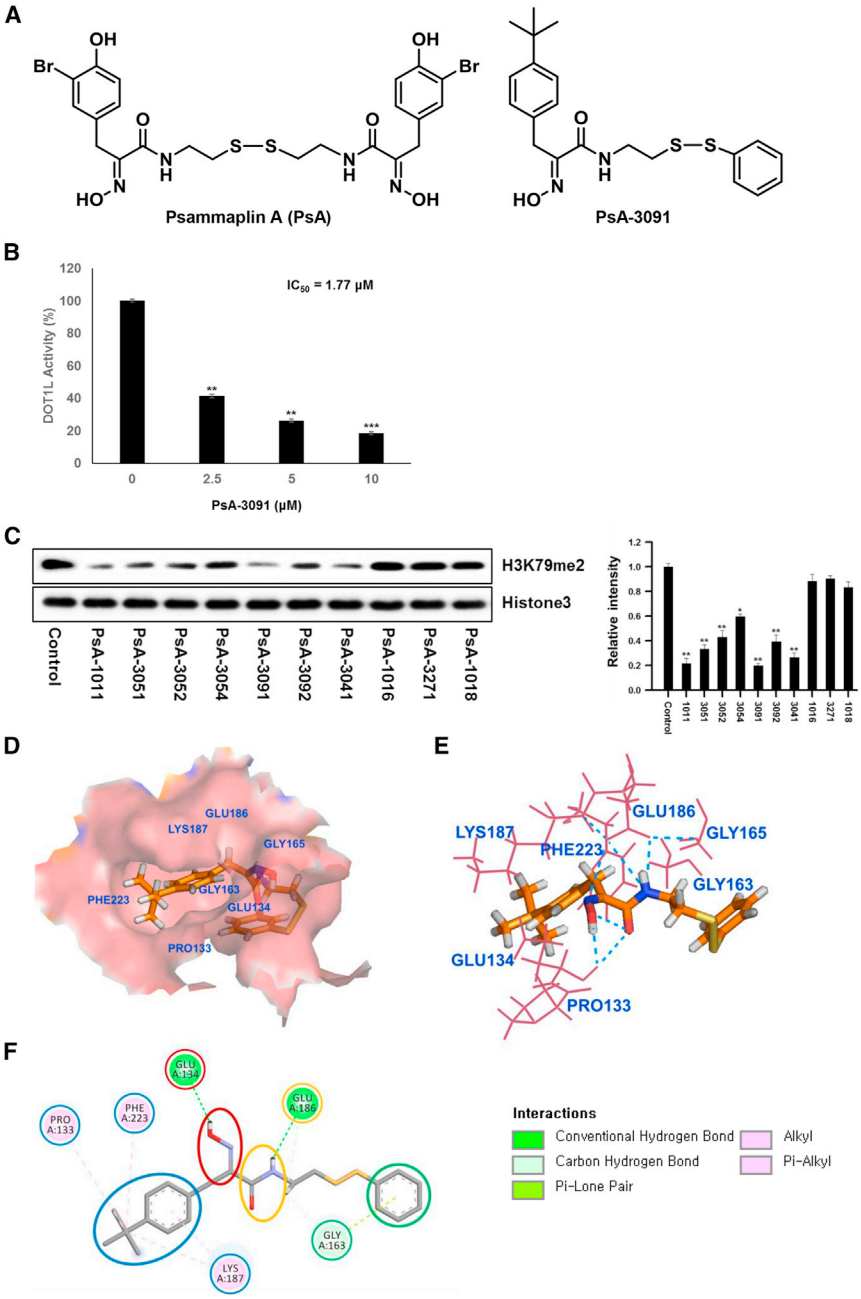

Figure 1. PsA Analogs Block the Methylation of Histone H3 Lysine 79 via Inhibition of DOT1L Activity

(A) The chemical structure of psammaplin A and PsA-3091. (B) The DOT1L enzyme assay was carried out using 500 ng DOT1L per well and incubated for 1 h. **p < 0.01; ***p < 0.001, compared with the control. (C) The cells were treated with the indicated concentrations of PsA analogs for 48 h, lysed, and subjected to western blotting. Histone H3 was used as an internal control. The relative intensity of the indicated proteins was semiquantified using NIH ImageJ software. The data are expressed as the mean values ± SD (n = 3) and are representative of three separate experiments. *p < 0.05; **p < 0.01, compared with the control. (D) PsA-3091 located in the deep and narrow binding pocket of human DOT1L (PDB: 3SR4). The *t*-butyl phenyl group of the ligand has hydrophobic interactions with Phe223 and Pro133, critical residues for the interaction with the adenosine moiety of SAM. (E) Interactions between PsA-3091 and key residues of human DOT1L with the hydrogen bonds are indicated with dotted lines. (F) Interaction diagram of PsA-3091 with the key residues in DOT1L.

DOT1L and E-cadherin Expression in Normal Breast Epithelial Cells and Breast Cancer Cells

Since the expression level of DOT1L is highly correlated with breast cancer progression and metastasis,[8] the expression levels of DOT1L and E-cadherin, an adhesion molecule in cell-cell junctions, in various types of breast cancer cell lines were determined by western blot analysis (Figure 2A). The cell lines of TNBCs (HCC38, HCC1937, MDA-MB-231, and Hs578T) were found to have higher expression levels compared with the breast epithelial cells (MCF10A) and non-TNBCs (SK-BR-3 and T-47D). Moreover, claudin-low-type (E-cadherin-low) TNBCs (MDA-MB-231 and Hs578T) showed a relatively high expression level of DOT1L compared with basal-type TNBCs (HCC38 and HCC1937). In addition, the expression level of E-cadherin was significantly low in the cell lines with high DOT1L expression (Figure 2A). Therefore, these two claudin-low-type TNBC cells (MDA-MB-231 and Hs578T) were selected to further elucidate the effects of PsA-3091 on the regulation of DOT1L-mediated functions in TNBCs. To obtain the clinical relevance of our data, we compared the mRNA expression levels of DOT1L in human TNBC, non-TNBC, and normal breast tissue samples available from public databases. The expression of DOT1L in TNBC (n = 116) was significantly higher than in both non-TNBC (n = 983, p = 4.97e−12) and normal breast tissue (n = 409, p = 3.47e−25), consistent with our cell-line results (Figure 2B). Furthermore, to confirm the relationship between the expression of DOT1L and the expression of E-cadherin, the MCF10A cells were transfected with lentiviral particles expressing DOT1L. As shown in Figure 2C, the expression of E-cadherin was downregulated by transduction of the DOT1L gene in MCF10A cells. We further confirmed that the knockdown of DOT1L by small interfering RNA (siRNA) augmented the expression of E-cadherin, and the co-treatment of DOT1L siRNA and PsA-3091 exhibited synergistic upregulation of E-cadherin expression in MDA-MB-231 cells (Figures 2D and 2E). In addition, the enhanced expression levels of DOT1L by the introduction of DOT1L-expressing lentiviral particles were abrogated for the effect

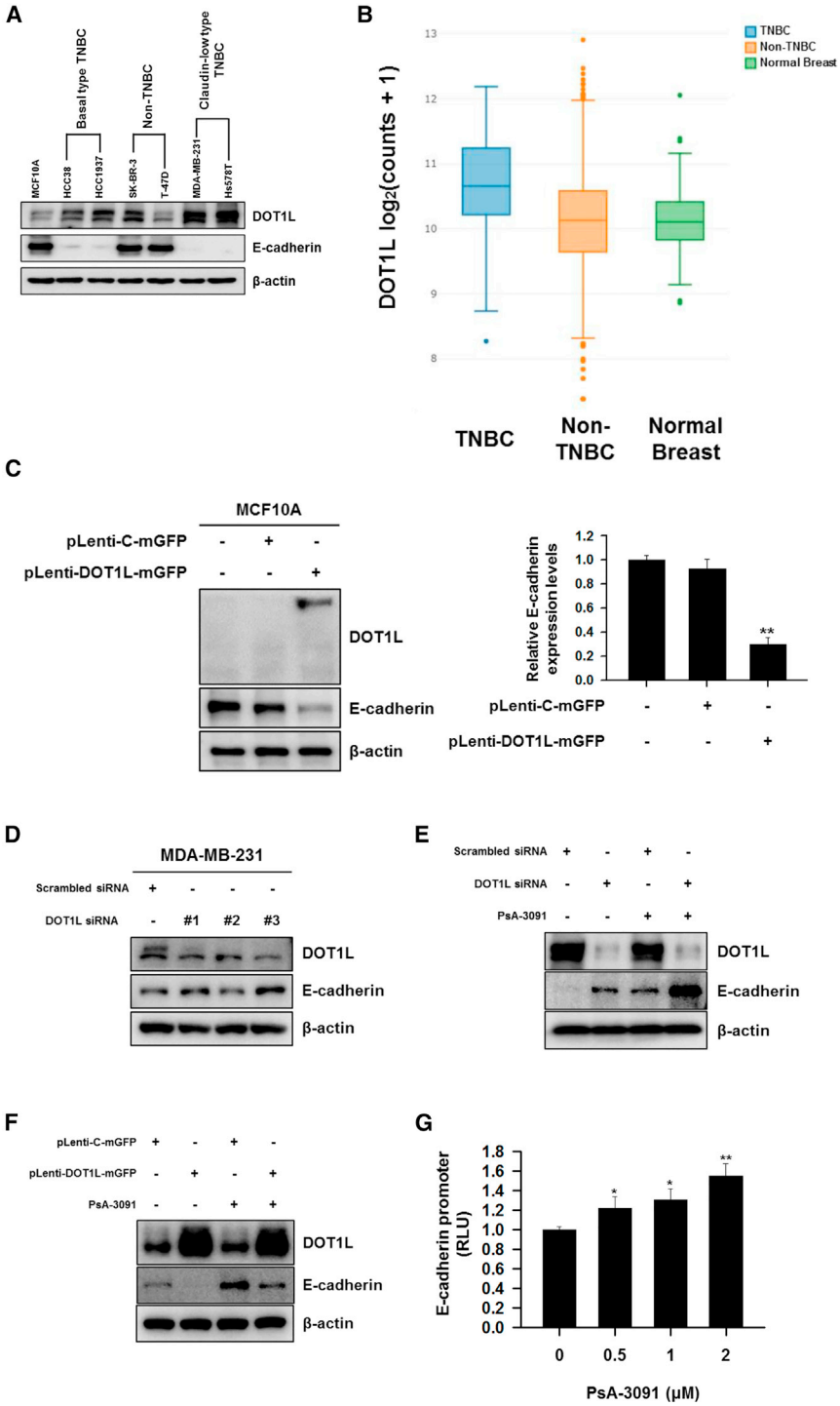

Figure 2. Expression Levels of DOT1L and E-cadherin Are Highly Correlated with Hormone Receptor Status in Breast Cancer Cells

(A) Western blotting analysis of DOT1L and E-cadherin expression in various breast cancer cell lines. β-Actin was used as an internal control. The relative intensity of the indicated proteins was semiquantified using NIH ImageJ software. (B) DOT1L expression in TNBCs compared to the non-TNBC and normal breast tissues based on TCGA and the GTex database. (C) Protein levels of DOT1L and E-cadherin in MCF10A cells that were transfected with empty or DOT1L expression lentiviral particles for 24 h. β-Actin was used as an internal control. The relative intensity of the indicated proteins was semiquantified using NIH ImageJ software. **$p < 0.01$, compared with the control. (D) The cells were transfected with negative control siRNA or DOT1L siRNA for 24 h. The cell lysates were immunoblotted with the indicated antibodies. (E) The cells were transfected with negative control siRNA or DOT1L siRNA for 48 h and treated with 1 μM PsA-3091 for an additional 48 h. The cell lysates were immunoblotted with the indicated antibodies. (F) The cells were transfected with empty or DOT1L expression lentiviral particles for 24 h and treated with 1 μM PsA-3091 for an additional 48 h. The cell lysates were immunoblotted with the indicated antibodies. (G) E-cadherin promoter activities were determined in MCF10A cells that were transfected with E-cad^{-108}-Luc and Renilla reporter gene plasmids for 24 h and subsequently incubated with PsA-3091 at the indicated concentrations for another 24 h. The results were normalized to the Renilla values and expressed as relative luciferase units (RLUs). The data are expressed as the mean values ± SD (n = 3) and are representative of three separate experiments. *$p < 0.05$; **$p < 0.01$, compared with the control.

of PsA-3091 on E-cadherin upregulation in MDA-MB-231 cells (Figure 2F). Moreover, treatment with PsA-3091 enhanced E-cadherin promoter activity in MCF10A cells (Figure 2G). These data support the notion that DOT1L expression is highly correlated with breast cancer cell metastasis by regulating E-cadherin expression and the possibility that PsA-3091 participates in the inhibition of metastasis by modulating E-cadherin expression in TNBCs.

Selective Inhibition of H3K79 Methylation and Suppression of Cell Proliferation by PsA-3091 in TNBC Cells

To further identify whether the inhibition of histone methylation by PsA-3091 was selective against DOT1L-mediated methylation of H3K79, the effects of PsA-3091 on the methylation of other histone H3 lysine residues were determined by western blot analysis. As shown in Figure 3A, PsA-3091 exhibited notable selective inhibitory effects on H3K79me2 over other lysine residues of histone H3 in both MDA-MB-231 and Hs578T human TNBC cells. Moreover, PsA-3091 showed increased inhibitory effects on DOT1L-mediated H3K79 methylation compared with PsA (Figure 3A). It is known that the selective inhibition of H3K79 di-methylation suppresses the proliferation and progression of breast cancer.[8] Therefore, a cell proliferation assay against

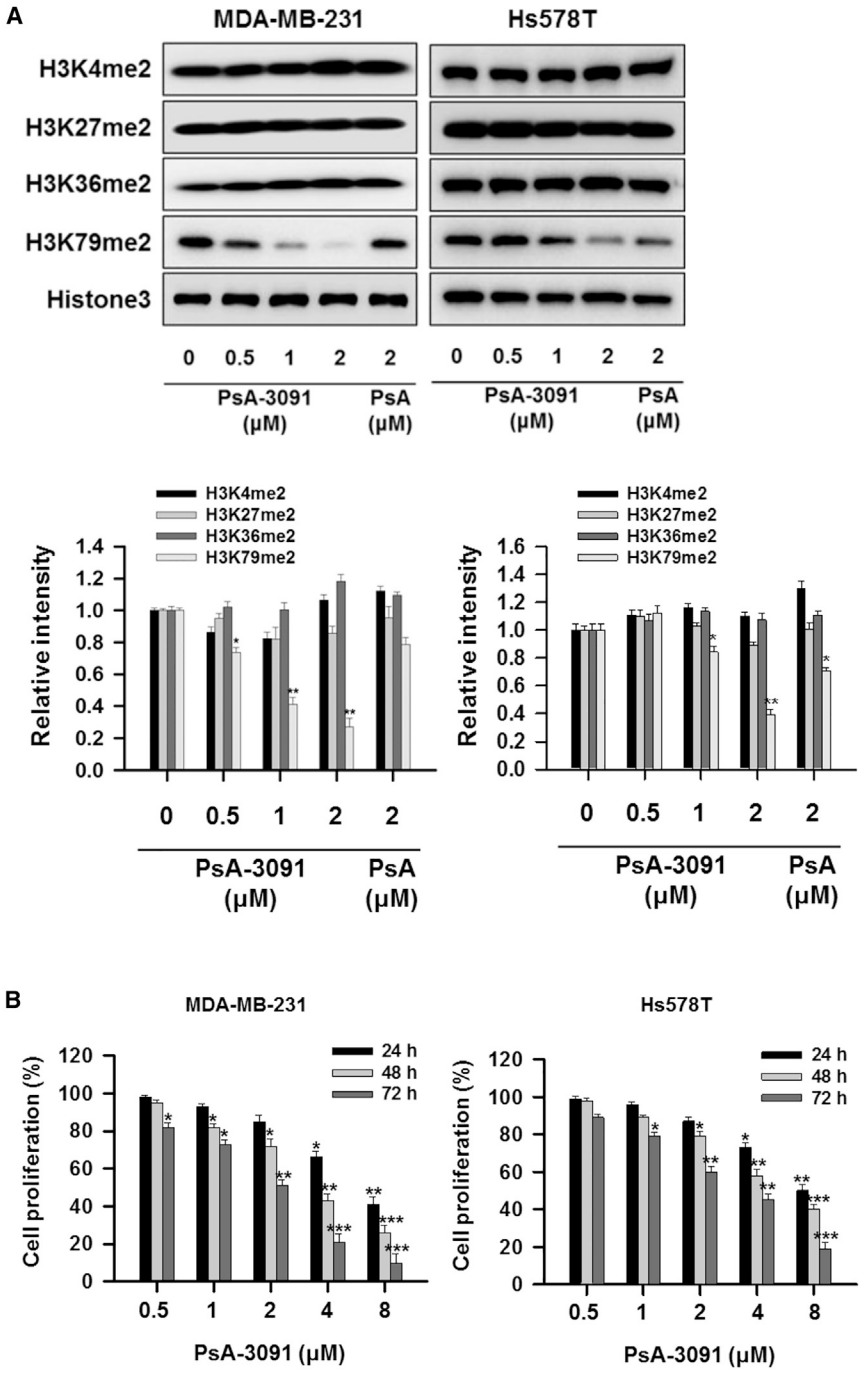

Figure 3. PsA-3091 Suppresses Cell Proliferation via Selective Inhibition of DOT1L in TNBC Cells

(A) The cells were treated with the indicated concentrations of PsA-3091 for 48 h, lysed, and subjected to western blotting. Histone H3 was used as an internal control. The relative intensity of the indicated proteins was semiquantified using NIH ImageJ software. *$p < 0.05$; **$p < 0.01$, compared with the control. (B) The cells were treated with PsA-3091 for the indicated times (24–72 h), and the proliferation of the cells was measured using the SRB assay. *$p < 0.05$; **$p < 0.01$; ***$p < 0.001$, compared with the control.

two selected TNBC cells was performed to identify whether the selective H3K79me2 inhibition by PsA-3091 was partly responsible for the anti-proliferative activity in TNBC cells. As shown in Figure 3B, PsA-3091 exhibited anti-proliferative activity in a concentration- and time-dependent manner in both TNBC cells with similar IC_{50} values (IC_{50} values of 2.14 μM for MDA-MB-231 cells and 2.21 μM for Hs578T cells, respectively, at the 72-h incubation). On the other hand, one of the nucleoside-type DOT1L inhibitors, EPZ-5676, exhibited an IC_{50} value over 50 μM in TNBC cells. To further determine whether the cytotoxicity is selective against cancer cells compared to normal cells, PsA-3091 was evaluated in a normal human breast epithelial cell (MCF10A). The IC_{50} values of PsA-3091 were over 141.25 μM against normal epithelial cell MCF10A, which showed over 60-fold higher cytotoxicity against cancer cells. Taken together, these data demonstrated that PsA-3091 could selectively inhibit the proliferation of TNBC cells via a regulation of the H3K79 methylation status.

Effects of PsA-3091 on DOT1L-Mediated Regulation of EMT Genes in Human Breast Cancer Cells

Accumulating evidence suggests that aberrant H3K79 methylation is responsible for the increased metastatic potential of breast cancers.[18] Therefore, the anti-metastatic activity of PsA-3091 was primarily estimated using wound healing and invasion assays to investigate whether the high metastatic potential of MDA-MB-231 and Hs578T cells was regulated by PsA-3091 treatment. As shown in Figures 4A and 4B, PsA-3091 treatment clearly suppressed wound closure and cell invasion through Matrigel-coated Transwell membranes in a concentration-dependent manner. To further explore the underlying molecular mechanisms of the inhibition of wound healing and cell invasion by PsA-3091, regulation of the EMT process, a key step in cancer metastasis, was examined in aggressive TNBC cells. Compared with the vehicle-treated group, the gain of expression of the epithelial biomarker E-cadherin and the loss of mesenchymal biomarkers such as N-cadherin, ZEB1, and vimentin were found in the PsA-3091-treated group at mRNA (Figure 4C) and protein (Figure 4D) levels. This finding suggests that PsA-3091 might have the potential to suppress the metastasis of breast cancer cells via DOT1L-mediated regulation of EMT pathways.

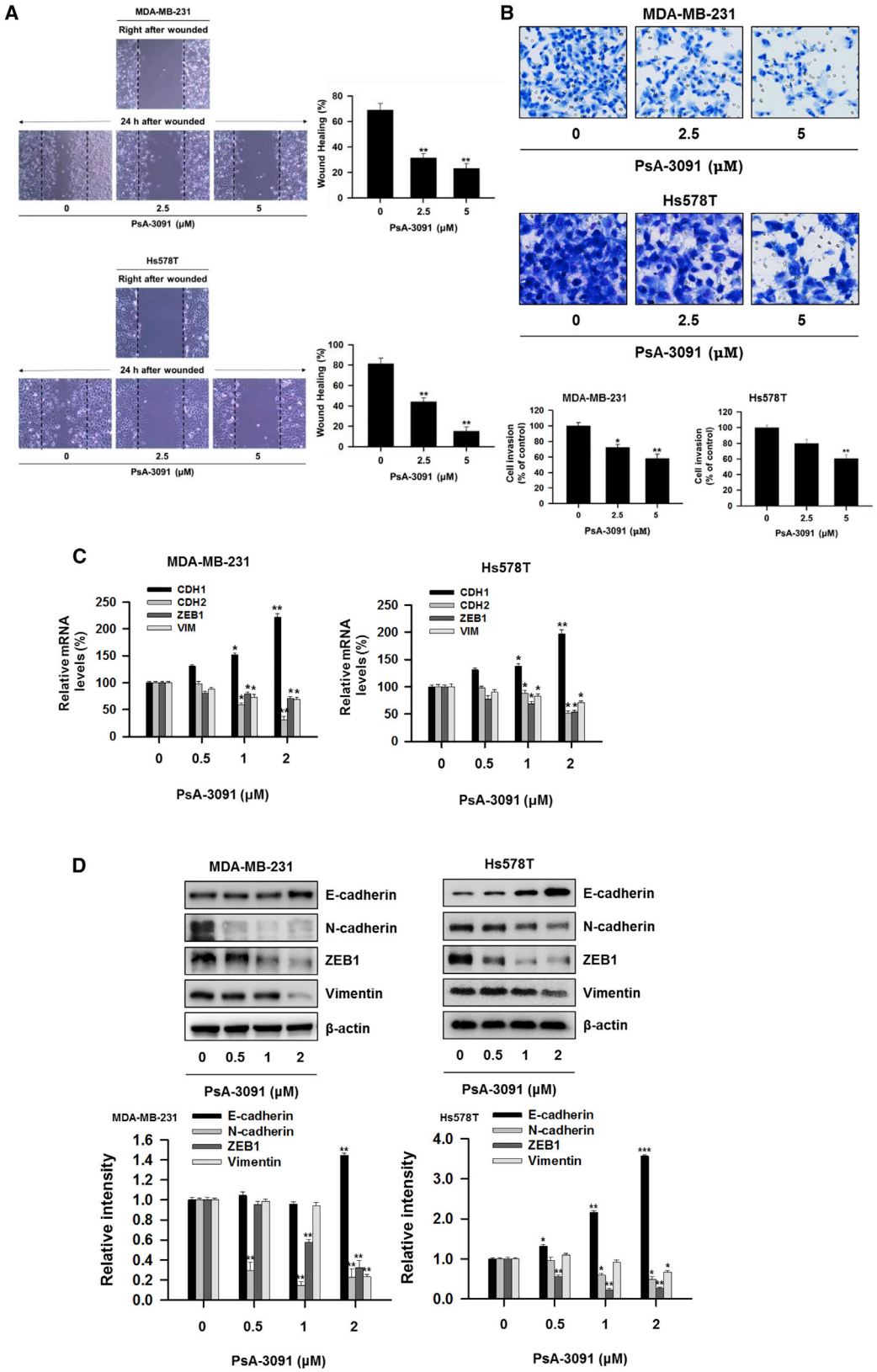

(legend on next page)

Antitumor and Anti-metastatic Activities of PsA-3091 in an Orthotopic Mouse Model

To determine whether the regulation of H3K79 methylation by PsA-3091 had a functional role in tumor growth and metastasis *in vivo*, we used an orthotopic mouse model implanted with MDA-MB-231/Luc cells (1×10^7 cells per mouse). When the primary tumor volume reached approximately 200 mm^3, either PsA-3091 (10 or 30 mg/kg), PsA (30 mg/kg), or paclitaxel (5 mg/kg, a positive control) was administered intraperitoneally (i.p.) three times a week for 38 days. In our previous study for antitumor activity of PsA and PsA analog against lung cancer cells, we found that the dose of 30 mg/kg of the test compounds was effective without overall toxicity.[25] Therefore, in this study, we also primarily selected the doses of 10 and 30 mg/kg to evaluate the dose-dependent activity in an *in vivo* orthotopic mouse model. The tumor growth in the PsA-3091-administered groups was significantly inhibited compared with that in the vehicle-treated control group. Moreover, PsA-3091 was found to be superior to PsA in the inhibition of tumor growth (Figure 5A). Similarly, the tumor weights measured on the last day of the experiment were 70.3% and 19.8% of the control weight (100%) for the 10- and 30-mg/kg PsA-3091 treatments, respectively (Figure 5B). No significant change in body weight was observed in the PsA-3091- or PsA-administered groups, while a significant loss of body weight was observed in the paclitaxel-administered group (Figure 5C). In addition, we also found that a single administration of PsA-3091 (300 mg/kg, p.o.) on ICR mouse did not show any obvious clinical symptoms of toxicity and mortality following 7 days of observation after administration (data not shown). These data suggest that the PsA-3091 might be considered to be relatively safe without acute toxicity in an *in vivo* animal model. Next, the optical images using IVIS were obtained to validate the primary tumor growth and incidence of organ metastasis. As shown in Figures 5D and 5E, the luciferase signal from the primary tumor site was decreased in the PsA-3091-administered groups, and spontaneous pulmonary metastasis was also significantly suppressed by PsA-3091 treatment.

Furthermore, histological H&E staining of lung tissues excised from the orthotopic mouse model also showed that the metastatic nodules in lung tissues were significantly suppressed by PsA-3091 treatment compared with the vehicle-treated control group (Figure 6A). These results demonstrate that PsA-3091 effectively inhibits the tumor growth and pulmonary metastasis of human breast cancer cells *in vivo*. To further validate whether the antitumor and anti-metastatic activities of PsA-3091 were associated with the inhibition of H3K79 methylation and regulation of the EMT process, additional biochemical analyses of tumor tissues were performed. Consistent with the *in vitro* findings, the mRNA and protein levels of vimentin and H3K79me2 were downregulated, while those of E-cadherin were upregulated by PsA-3091 treatment in a concentration-dependent manner (Figures 6B and 6C). Immunochemical analysis of the primary tumor tissues also suggested that PsA-3091 effectively inhibited the expression levels of Ki67, a cell proliferation biomarker, and H3K79me2. Moreover, PsA-3091 augmented the expression levels of E-cadherin while inhibiting the expression of vimentin (Figure 6D). Taken together, these data confirm that PsA-3091 suppresses *in vivo* tumor growth and metastasis of breast cancer cells into lung tissues by regulating H3K79 methylation and DOT1L-mediated EMT markers.

DISCUSSION

Metastatic breast cancer, which has high metastatic potential to other organs in the body, is of major concern as a causal factor for cancer death in women.[28–30] Recent studies have indicated that the aggressive and highly metastatic characteristics of breast cancer are, in part, associated with the aberrant methylation of histone H3 lysine 79 (H3K79me2) mediated by a histone methyltransferase, DOT1L.[18] Therefore, approaches to developing inhibitors for DOT1L in breast cancer are actively being studied. However, the effects of early developed nucleoside-containing DOT1L inhibitors on solid cancers were not sufficient compared with the effects of the compounds on MLL-rearranged leukemia.[27] In our previous study, we proposed a new, precise method for the synthesis of PsA and its analogs, and we demonstrated that the disulfide group and free oxime group are essential for cytotoxicity against a panel of cancer cells. We also revealed that a β-naphthyl-substituted homodimeric analog exhibited HDAC-inhibitory activity in lung cancer cells.[25] Based on these findings, we developed and found that PsA-3091, a heteromonomeric structured analog with a tertiary butyl functional group, showed effective antitumor and anti-metastatic activities in both *in vitro* cell cultures and *in vivo* animal models, being the most effective among the analogs of PsA for the inhibition of DOT1L activity. Interestingly, heteromonomeric structured analogs were effective for the suppression of DOT1L, while homodimeric structured analogs were effective on the inhibition of HDAC. It was found that PsA-3091 could suppress the methylation of H3K79 without altering the methylation status of other histone H3 lysine residues such as H3K4, H3K27, and H3K36. We also

Figure 4. PsA-3091 Suppresses Cell Migration and Invasion via the Regulation of the EMT Process in TNBC Cells

(A) After mechanically generating scratches in monolayers of MDA-MB-231 and Hs578T cells, cells were treated with PsA-3091 for 24 h, and representative images of wound closure were observed under a light microscope (left). The area of the wound was quantified using NIH ImageJ software (right). $^{**}p < 0.01$, compared with the control. (B) The cells were pretreated with PsA-3091 at the indicated concentrations for 24 h, and the cells were reseeded into the upper chambers of the Transwell and incubated for 24 h. Invaded cells were fixed, stained, imaged (top), and counted (bottom). $^{*}p < 0.05$; $^{**}p < 0.01$, compared with the control. (C) The cells were treated with PsA-3091 at the indicated concentrations for 24 h, and the mRNA levels of E-cadherin (CDH1), N-cadherin (CDH2), ZEB1, and vimentin (VIM) were examined using real-time PCR. $^{*}p < 0.05$, $^{**}p < 0.01$ compared with the control. (D) Expression levels of EMT in MDA-MB-231 and Hs578T cells that were treated with PsA-3091 for 48 h were detected by western blot analysis using β-actin as an internal control. The relative intensity of the indicated proteins was semiquantified using NIH ImageJ software. The data are expressed as the mean values ± SD (n = 3) and are representative of three separate experiments. $^{*}p < 0.05$; $^{**}p < 0.01$; $^{***}p < 0.001$, compared with the control.

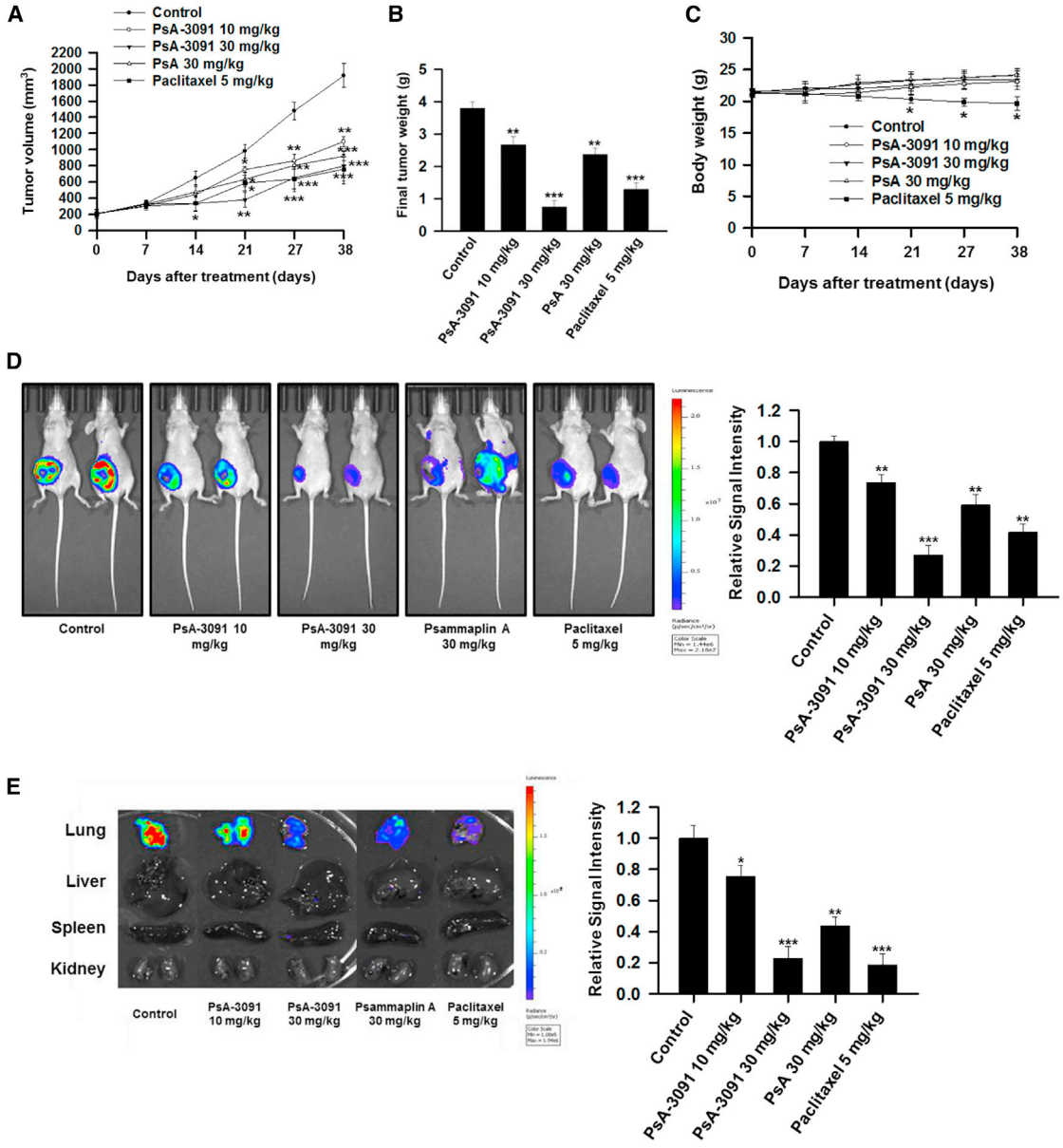

Figure 5. PsA-3091 Inhibits Tumor Growth and Pulmonary Metastasis in an Orthotopic Mouse Model Implanted with MDA-MB-231 Cells

(A) Tumor volumes of the MDA-MB-231 orthotopic mouse model, which were administered intraperitoneally three times per week with vehicle, PsA-3091 (10 or 30 mg/kg), PsA (30 mg/kg), and paclitaxel (5 mg/kg) for 38 days, were measured every 3 days with a caliper. (B) Primary tumors were excised from mice at the termination of the experiment, and tumor weights were measured. (C) Body weights of the mice were measured every 7 days. (D) Luciferase imaging (IVIS) of BALB/c nude mice on the last day of the experiment. Each group of mice was administered the indicated concentrations of each compound. Relative signal intensity was quantified using PerkinElmer Living Image software. (E) Organs (lung, liver, spleen, and kidney) of the mice were excised at the termination of the experiment and imaged by IVIS. Relative signal intensity was quantified using PerkinElmer Living Image software. *$p < 0.05$; **$p < 0.01$; ***$p < 0.001$, compared with control.

revealed that interactions between the binding site of DOT1L and PsA-3091 might interfere with the interaction between DOT1L and SAM.

The methylation of histone H3 lysine residues by HMTs has recently been found to be a potential target for cancer therapies.[31–33] For instance, the inhibition of EZH2, a specific methyltransferase for H3K27me3, can effectively suppress tumor growth by inducing cell-cycle arrest.[34] In particular, DOT1L, a specific methyltransferase for H3K79, plays a crucial role in tumor development and metastasis by mediating the transcription of its target genes.[8,35] Previous studies have reported that (1) aberrant H3K79 methylation by DOT1L is

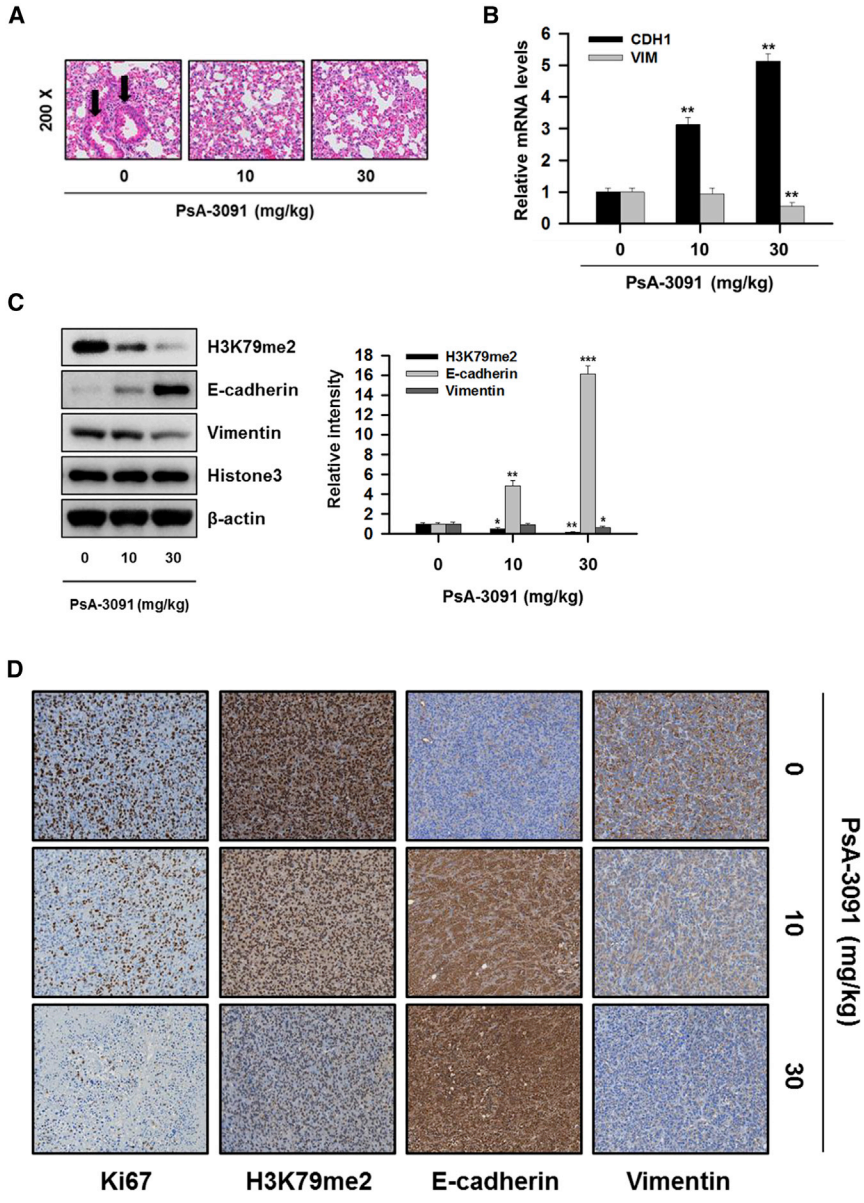

Figure 6. PsA-3091 Regulates the Expression of EMT Genes *In Vivo* via the Inhibition of H3K79 Methylation in Tumor Tissues

(A) Representative H&E staining of pulmonary metastasis from lungs in orthotopically transplanted nude mice; arrow indicates metastatic nodules. (B) Total RNA was extracted from excised tumor tissues, and the mRNA levels of E-cadherin (CDH1) and vimentin (VIM) were determined by real-time PCR analysis. (C) Small portions of tumors from each group were homogenized in complete lysis buffer (Active Motif, Carlsbad, CA, USA). The expression levels of E-cadherin and vimentin and the methylation levels of H3K79 were determined by western blot analysis using antibodies against E-cadherin, vimentin, and H3K79me2. β-Actin and histone H3 were used as internal controls. The relative intensity of the indicated proteins was semiquantified using NIH ImageJ software. (D) Immunohistochemical analyses of Ki67, H3K79me2, E-cadherin, and vimentin were performed using antibodies against each protein in MDA-MB-231/Luc tumor sections. Sections were counterstained with hematoxylin and imaged with the Vectra 3.0 Imaging System (PerkinElmer, 200×). The data are expressed as the mean values ± SD (n = 3) and are representative of three separate experiments. *$p < 0.05$; **$p < 0.01$; ***$p < 0.001$, compared with the control.

related to the development of MLL-rearranged leukemia; (2) DOT1L is involved in sphere formation and cell migration by regulating the expression of BCAT1; and (3) DOT1L regulates CDH1 transcription by cooperating with the c-*myc*-p300 complex.[8,15,35] However, the expression level of DOT1L in various breast cancers with different hormone receptor statuses has not yet been investigated. Additionally, the survival rate of breast cancer patients is highly correlated with the hormone receptor subtype and metastasis status.[36,37] Herein, the expression levels of DOT1L and E-cadherin were evaluated in various types of breast cell lines, including breast epithelial cells, non-TNBCs, and two different types of TNBCs. Interestingly, claudin-low-type TNBCs (MDA-MB-231 and Hs578T) were found to exhibit higher expression of DOT1L, while the expression of E-cadherin was almost abolished. Moreover, the introduction of DOT1L genes in MCF10A cells was found to decrease the expression of E-cadherin. This result strengthens the involvement of DOT1L in the regulation of E-cadherin expression.

It is known that EMT is the key regulator and plays a crucial role in cancer metastasis.[38,39] In addition, recent studies have revealed that the EMT process in breast cancer is partly regulated by epigenetic programs.[8,9] As the role of DOT1L in the regulation of the EMT process and its relation to breast cancer metastasis have been previously reported, overexpression of DOT1L could be a biomarker in TNBCs. In the present study, we showed that the expression levels of EMT markers, including E-cadherin, N-cadherin, ZEB1, and vimentin, in breast cancer cells were notably regulated by treatment with PsA-3091. The regulation of EMT markers by PsA-3091 consequently suppressed the migration and invasion of breast cancer cells, which might be partly associated with the anti-metastatic activity of PsA-3091. In particular, spontaneous pulmonary metastasis from primary tumors in an *in vivo* animal model was significantly suppressed by PsA-3091 treatment.

In summary, the present findings suggest that the expression of DOT1L is highly correlated with the hormone receptor status of breast cancers and is concerned with high metastatic potential

mediated by the EMT process in TNBCs. Furthermore, we found that a new template of the DOT1L inhibitor, PsA-3091, exhibits significant antitumor and anti-metastatic activities both *in vitro* and *in vivo*. These findings may be significant not only because this is the first report of non-nucleoside types of DOT1L inhibitor with the anti-metastatic activity but also because DOT1L may be a potential target for metastatic breast cancer.

MATERIALS AND METHODS

Cell Culture and Chemicals

Human breast cancer cells (MDA-MB-231, Hs578T, HCC38, HCC1937, SK-BR-3, and T-47D) and human breast epithelial cells (MCF10A) were obtained from the American Type Culture Collection (Manassas, VA, USA). The cells were cultured in medium (DMEM for MDA-MB-231, Hs578T, and SK-BR-3 cells; RPMI 1640 for HCC38, HCC1937, and T-47D cells; and DMEM: Nutrient Mixture F-12 for MCF10A) supplemented with antibiotics-antimycotics (PSF: 100 U/mL sodium penicillin G, 100 μg/mL streptomycin, and 250 ng/mL amphotericin B) and 10% fetal bovine serum (FBS) in an incubator containing 5% CO_2 at 37°C. All reagents used for cell culture were purchased from GIBCO-Invitrogen (Grand Island, NY, USA). Paclitaxel and sulforhodamine B (SRB) were purchased from Sigma-Aldrich (St. Louis, MO, USA). Analogs of PsA were provided by co-author H.-g. Park. The stock solutions were dissolved in 100% DMSO.

DOT1L (KMT4) Enzyme Assay

The DOT1L enzyme activity was measured using concentrations of 5 μM SAM as the methyl group donor, synthesized DOT1L substrate as the substrate, and 25 ng/μL DOT1L enzyme from BPS Bioscience (catalog no. 52202; San Diego, CA, USA) according to the manufacturers' instructions.

Western Blot Analysis

Total cell lysates were prepared in 2× sample loading buffer (250 mM Tris-HCl [pH 6.8], 10% glycerol, 4% SDS, 2% β-mercaptoethanol, 0.006% bromophenol blue, 5 mM sodium orthovanadate, and 50 mM sodium fluoride; Bio-Rad). The protein concentrations of samples were measured using the bicinchoninic acid method.[40] Equal amounts of protein (520 μg) were separated by 8%–15% SDS-PAGE and transferred to polyvinylidene fluoride membranes (Millipore, Bedford, MA, USA).[41] The membranes were blocked with 5% BSA (Sigma-Aldrich) and then probed with anti-E-cadherin, anti-N-cadherin (BD Biosciences), anti-DOT1L, anti-H3K4me2, anti-H3K27me2, anti-H3K36me2, anti-H3K79me2, anti-Histone H3 (Cell Signaling Technology, Beverly, MA, USA), anti-ZEB1, anti-vimentin, or anti-β-actin (Santa Cruz Biotechnology, Dallas, TX, USA) antibodies. The blots were detected with an enhanced chemiluminescence (ECL) detection kit (GE Healthcare, Little Chalfont, UK).

Molecular Docking Analysis

Molecular docking analysis was conducted using the SYBYL-X 2.1.1 (Tripos International, St. Louis, MO, USA) with Surflex-Dock GeomX mode. The crystal structure of human DOT1L with a selective inhibitor, TT8, was used for docking (PDB: 3SR4). The new ligand, PsA-3091, was prepared by generating 3D Concord conformations from the 2D structure, and the energy was minimized using Powell's method until the gradient converged to a value of 0.001 kcal/mol • Å. The prepared ligand was docked into the crystal structure of human DOT1L. Staged minimization of the protein was performed using Powell's method until the termination gradient was lower than 0.5 kcal/mol • Å. All water molecules were removed, and ProtoMol was generated based on the location of the original ligand, TT8, with a threshold of 0.5 Å and bloat of 0 Å. The protein flexibility option in the binding pocket was used to allow protein movement. Docking performance was validated by the docking scores, visual inspections, and the root-mean-square deviation (RMSD) value of the redocked poses compared with the original structure. Further analyses of the molecular interactions between the ligand and protein were conducted using the Discovery Studio 4.5 Visualizer (Biovia, San Diego, CA, USA) and PyMOL v1.0 (Schrödinger, Tokyo, Japan).

Comparison of the DOT1L Gene Expression in TNBC, Non-TNBC, and Normal Breast Tissues in Human Samples

The mRNA expression levels (RSEM expected count, DESeq2 standardized) were obtained from The Cancer Genome Atlas (TCGA), the Genotype-Tissue Expression (GTEx) database, and tumor alterations relevant for genomics-driven therapy (TARGET) data retrieved from the Xena portal site (http://xena.ucsc.edu/),[42] and the IDs were matched using the respective mapping files. The TNBC status was identified using the disease-related information of the The Cancer Genome Atlas Breast Invasive Carcinoma (TCGA-BRCA) project available from the NIH National Cancer Institute GDC Data Portal (https://portal.gdc.cancer.gov/). Statistical analyses between groups were performed using R v3.5.2 with Student's t test or Welch's t test, depending on the p value of prior F tests (threshold $p = 0.05$). Boxplots were drawn using the "Plotly" package (Collaborative Data Science; Plotly Technologies, Montréal, QC, Canada; https://plot.ly/).

Lentiviral Transduction

Lentiviral particles expressing the full-length DOT1L cDNA clone were purchased from OriGene Technologies (Rockville, MD, USA), and the sequence was verified to be 100% identical to the published sequence, NCBI: NM_032482. For transient transduction, cells were transduced with 1 μg pLenti-C-mGFP or pLenti-DOT1L-mGFP using TurboFectin 8.0 (OriGene Technologies, Rockville, MD, USA), according to the manufacturer's instructions.

RNAi

RNAi of *DOT1L* was performed using 19-bp siRNA duplexes purchased from Bioneer (Daejeon, Korea). The coding strands for *DOT1L* were as follows: #1, 5′-CAG UGA UGG UGC UUC UCU U-3′; #2, 5′-GAA GUG GAU GAA AUG GUA U-3′; #3, 5′-GAC CUG AUU CAA GCG CAG A-3′. The cells were transfected with 20 nM siRNA duplexes using Lipofectamine RNAiMAX (Invitrogen, Carlsbad, CA, USA) according to the manufacturer's instructions. Cells transfected with a control nonspecific siRNA duplex (Invitrogen, Carlsbad, CA, USA) were used as controls for direct comparison.

E-cadherin Reporter Gene Assay

The wild-type and E-box mutant *E-cadherin* reporter gene plasmids, E-cad^{-108}-Luc and E-cad^{-108}-EboxA^{MT}-EboxB^{MT}-EboxC^{MT}-Luc (E-cad^{-108} 3× MT), and wild-type expression vectors were gifts from Dr. J.I. Yook (Yonsei University, Seoul, Korea).[43] MCF10A cells (5×10^4 cells per well) were seeded in 48-well plates. After 24 h of incubation, the cells were transfected with 40 ng wild- or mutant-type E-cad^{-108}-Luc and 1 ng *Renilla* luciferase vector. Transient transfections were performed using Lipofectamine 2000 (Invitrogen, Carlsbad, CA, USA). At 24 h after plasmid transfection, the cells were treated with a test compound or with a control, DMSO (Sigma-Aldrich), for an additional 24 h. Then, the cell lysates were subjected to the dual luciferase activity assay using the Dual Luciferase Reporter Assay System (Promega, Madison, WI, USA), according to the manufacturer's instructions. Luciferase activities were normalized to the *Renilla* values and are presented as the relative luciferase activity.[44]

Cell Proliferation Assay

Cell proliferation was measured by the SRB assay.[45] Briefly, cells were seeded in 96-well plates and incubated for 30 min (for 0-day controls) or treated with test compounds for the indicated times. After incubation, the cells were fixed, dried, and stained with 0.4% SRB in 1% acetic acid solution. Unbound dye was removed by washing, and stained cells were dissolved in 10 mM Tris (pH 10.0). The absorbance was measured at 515 nm, and cell proliferation was determined. IC_{50} values were calculated by nonlinear regression analysis using TableCurve 2D v5.01 software (Systat Software, San Jose, CA, USA). All reagents were purchased from Sigma-Aldrich.

Wound Healing Assay

MDA-MB-231 and Hs578T cells were grown to 80%–90% confluence in a 6-well plate. A confluent monolayer of the cells was artificially wounded with a 200-μL pipette tip, and the detached cells were washed with PBS (Invitrogen), followed by incubation with 1% FBS in medium containing various concentrations of compound for 24 h. The wounds were photographed at 0 and 24 h on an inverted microscope (Olympus, Tokyo, Japan). The wound area was quantified using ImageJ software (NIH) and presented as the wound healing (%) in comparison to the area of the wound at 0 h.[46]

Cell Invasion Assay

Twenty-four-well Transwell membrane inserts with 6.5-mm diameters and 8-μm pore sizes (Corning, Tewksbury, MA, USA) were coated with 10 μL type I collagen (0.5 mg/mL, BD Biosciences, San Diego, CA, USA) and 20 μL of a 1:20 mixture of Matrigel (BD Biosciences)/PBS. After treatment with the compounds for 24 h, MDA-MB-231 and Hs578T cells were harvested, resuspended in serum-free medium, and plated ($0.5–1 \times 10^6$ cells per chamber) in the upper chamber of the Matrigel-coated Transwell insert. Medium containing 30% FBS was used as a chemoattractant in the lower chambers. After 24 h of incubation, the cells that had invaded the outer surface of the lower chambers were fixed and stained using the Diff-Quik Staining Kit (Sysmex, Kobe, Japan) and imaged. Representative images from 3 separate experiments are shown, and the number of invaded cells was counted in 5 randomly selected microscopic fields (magnification, 200×).[47]

RNA Isolation and Real-Time PCR

The total RNA from the cells was extracted with TRIzol Reagent (Invitrogen, Carlsbad, CA, USA), and 1 μg total RNA was reverse-transcribed using the Reverse Transcription System (catalog no. A3500; Promega, Madison, WI, USA) according to the manufacturer's instructions. Real-time PCR was conducted using iQ SYBR Green Supermix (Bio-Rad, Hercules, CA, USA) according to the manufacturer's instructions. The threshold cycle (C_T) was determined using Bio-Rad CFX Manager 3.1 software. Relative quantification between compounds and untreated controls normalized to the levels of β-actin mRNA was calculated using the comparative C_T method.[44] The following primers were used for real-time PCR: *CDH1*, 5′-GTT ATT CCT CTC CCA TCA GCT G-3′ and 5′-CTT GGC TGA GAG GAT GGT GTA A-3′; *CDH2*, 5′-AGC CAA CCT TAA CTG AGG AGT-3′ and 5′-GGC AAG TTG ATT GGA GGG ATG-3′; *ZEB1*, 5′- GCA CCT GAA GAG GAC CAG AG-3′ and 5′-GTG TAA CTG CAC AGG GAG CA-3′; *VIM*, 5′-AGA TGG CCC TTG ACA TTG AG-3′ and 5′-TGG AAG AGG CAG AGA AAT CC-3′; *DOT1L/KMT4*, 5′-GGA GCT GGG CGT TCT TCT-3′ and 5′-GCA GTT CCT GGC ATA CAC AA-3′; *β-actin,* 5′-AGC ACA ATG AAG ATC AAG AT-3′ and 5′-TGT AAC GCA ACT AAG TCA TA-3′.

In Vivo Orthotopic Mouse Tumor Model

All animal experiments were conducted following the guidelines approved by the Seoul National University Institutional Animal Care and Use Committee (IACUC; permission number: SNU-170912-13). Female nude mice (BALB/c-nu), 5–6 weeks old, were purchased from Central Laboratory Animal (Seoul, Korea) and housed under pathogen-free conditions with a 12-h:12-h light:dark schedule. Luciferase-expressing MDA-MB-231 cells were inoculated orthotopically into the fourth fat pad of mice (1×10^7 cells in 100 μL 50:50 DMEM/Matrigel) using a 29G needle.[48] Ten days after implantation, the mice were randomized into the vehicle control and treatment groups, with six animals per group, and were administered vehicle (EtOH/Cremophor/normal saline = 5:5:90), PsA-3091 (10 or 30 mg/kg body weight), PsA (30 mg/kg), or paclitaxel (5 mg/kg body weight, Sigma-Aldrich) as a positive reference control. Compounds were administered i.p. three times per week for 38 days. An additional week later, anesthetized mice were positioned in the IVIS (PerkinElmer, Waltham, MA, USA) and imaged 15 min after injection of D-luciferin (150 mg/kg, Gold Biotechnology) resuspended in PBS. Mice were euthanized, and primary tumors and organs (lung, liver, spleen, kidney) were excised, weighed, and frozen for further biochemical analysis or fixed for immunohistochemistry. The length (L), width (W), and height (H) of the tumors were also measured using a digital slide caliper once a week, and tumor volumes (in cubic millimeters) were estimated by the formula LWH/2. Toxicity was assessed based on the lethality and body weight loss exhibited by the nude mice.

Ex Vivo Immunohistochemistry and Biochemical Analyses of Tumors

Tumor tissues fixed in 4% paraformaldehyde (PFA) were embedded in paraffin, sectioned and mounted on slides, deparaffinized with xylene, rehydrated with an ethanol series, and subjected to antigen retrieval. The slides were incubated with the indicated antibodies, which were detected using the LSAB$^+$ System-HRP Kit (Dako, Glostrup, Denmark), and counterstained with hematoxylin. Stained sections were observed and imaged using a Vectra 3.0 Automated Quantitative Pathology Imaging System (PerkinElmer, Waltham, MA, USA). A portion of the frozen tumors excised from nude mice was homogenized using a hand-held homogenizer in Complete Lysis Buffer (Active Motif, Carlsbad, CA, USA) or TRIzol Reagent (Invitrogen, Carlsbad, CA, USA). The mRNA and protein expression levels of the tumor lysates were determined. The protein concentrations of tumor lysates were measured using the Bradford assay.[49]

Statistical Analysis

The data are presented as the mean values ± SD for the indicated number of independently performed experiments. All data are representative of the results of at least three independent experiments. The statistical significance was analyzed using Student's t test or one-way ANOVA coupled with Dunnett's t test. Differences were considered statistically significant at $^*p < 0.05$, $^{**}p < 0.01$, and $^{***}p < 0.001$.

AUTHOR CONTRIBUTIONS

W.S.B. and S.K.L. designed experiments and wrote the manuscript. W.S.B. performed most of the experiments and analyzed the data. W.K.K., H.-J.C., S.K., D.K., and E.S.B. assisted in the *in vivo* experiments. H.S.K. and S.P. analyzed gene expression from TCGA and the GTex database. K.J. and J.L. performed the docking assay. H.J.H. and H.-g.P. designed and contributed psammaplin A analogs. All authors read and approved the final manuscript.

CONFLICTS OF INTEREST

The authors declare no competing interests.

ACKNOWLEDGMENTS

We thank Dr. Ho-Young Lee for providing the luciferase-expressing MDA-MB-231 cell lines. This study was supported by a National Research Foundation of Korea (NRF) grant funded by the Korean government (NRF-2016M3A9B6903499).

REFERENCES

1. Jamdade, V.S., Sethi, N., Mundhe, N.A., Kumar, P., Lahkar, M., and Sinha, N. (2015). Therapeutic targets of triple-negative breast cancer: a review. Br. J. Pharmacol. *172*, 4228–4237.

2. Guiu, S., Mollevi, C., Charon-Barra, C., Boissière, F., Crapez, E., Chartron, E., Lamy, P.J., Gutowski, M., Bourgier, C., Romieu, G., et al. (2018). Prognostic value of androgen receptor and FOXA1 co-expression in non-metastatic triple negative breast cancer and correlation with other biomarkers. Br. J. Cancer *119*, 76–79.

3. Bos, P.D., Zhang, X.H., Nadal, C., Shu, W., Gomis, R.R., Nguyen, D.X., Minn, A.J., van de Vijver, M.J., Gerald, W.L., Foekens, J.A., and Massagué, J. (2009). Genes that mediate breast cancer metastasis to the brain. Nature *459*, 1005–1009.

4. Lee, E., Pandey, N.B., and Popel, A.S. (2014). Pre-treatment of mice with tumor-conditioned media accelerates metastasis to lymph nodes and lungs: a new spontaneous breast cancer metastasis model. Clin. Exp. Metastasis *31*, 67–79.

5. Geng, S.Q., Alexandrou, A.T., and Li, J.J. (2014). Breast cancer stem cells: multiple capacities in tumor metastasis. Cancer Lett. *349*, 1–7.

6. Wu, Y.S., Lee, Z.Y., Chuah, L.H., Mai, C.W., and Ngai, S.C. (2019). Epigenetics in metastatic breast cancer: its regulation and implications in diagnosis, prognosis and therapeutics. Curr. Cancer Drug Targets *19*, 82–100.

7. Rifaï, K., Idrissou, M., Penault-Llorca, F., Bignon, Y.J., and Bernard-Gallon, D. (2018). Breaking down the contradictory roles of histone deacetylase SIRT1 in human breast cancer. Cancers (Basel) *10*, E409.

8. Cho, M.H., Park, J.H., Choi, H.J., Park, M.K., Won, H.Y., Park, Y.J., Lee, C.H., Oh, S.H., Song, Y.S., Kim, H.S., et al. (2015). DOT1L cooperates with the c-Myc-p300 complex to epigenetically derepress CDH1 transcription factors in breast cancer progression. Nat. Commun. *6*, 7821.

9. Dong, C., Wu, Y., Yao, J., Wang, Y., Yu, Y., Rychahou, P.G., Evers, B.M., and Zhou, B.P. (2012). G9a interacts with Snail and is critical for Snail-mediated E-cadherin repression in human breast cancer. J. Clin. Invest. *122*, 1469–1486.

10. Dong, C., Yuan, T., Wu, Y., Wang, Y., Fan, T.W., Miriyala, S., Lin, Y., Yao, J., Shi, J., Kang, T., et al. (2013). Loss of FBP1 by Snail-mediated repression provides metabolic advantages in basal-like breast cancer. Cancer Cell *23*, 316–331.

11. Nguyen, A.T., and Zhang, Y. (2011). The diverse functions of Dot1 and H3K79 methylation. Genes Dev. *25*, 1345–1358.

12. Hyun, K., Jeon, J., Park, K., and Kim, J. (2017). Writing, erasing and reading histone lysine methylations. Exp. Mol. Med. *49*, e324.

13. Kim, W., Choi, M., and Kim, J.E. (2014). The histone methyltransferase Dot1/DOT1L as a critical regulator of the cell cycle. Cell Cycle *13*, 726–738.

14. Valencia-Sánchez, M.I., De Ioannes, P., Wang, M., Vasilyev, N., Chen, R., Nudler, E., Armache, J.P., and Armache, K.J. (2019). Structural basis of Dot1L stimulation by histone H2B lysine 120 ubiquitination. Mol. Cell *74*, 1010–1019.e6.

15. Bernt, K.M., Zhu, N., Sinha, A.U., Vempati, S., Faber, J., Krivtsov, A.V., Feng, Z., Punt, N., Daigle, A., Bullinger, L., et al. (2011). MLL-rearranged leukemia is dependent on aberrant H3K79 methylation by DOT1L. Cancer Cell *20*, 66–78.

16. Nguyen, A.T., Taranova, O., He, J., and Zhang, Y. (2011). DOT1L, the H3K79 methyltransferase, is required for MLL-AF9-mediated leukemogenesis. Blood *117*, 6912–6922.

17. Skucha, A., Ebner, J., Schmöllerl, J., Roth, M., Eder, T., César-Razquin, A., Stukalov, A., Vittori, S., Muhar, M., Lu, B., et al. (2018). MLL-fusion-driven leukemia requires SETD2 to safeguard genomic integrity. Nat. Commun. *9*, 1983.

18. Zhang, L., Deng, L., Chen, F., Yao, Y., Wu, B., Wei, L., Mo, Q., and Song, Y. (2014). Inhibition of histone H3K79 methylation selectively inhibits proliferation, self-renewal and metastatic potential of breast cancer. Oncotarget *5*, 10665–10677.

19. Zhang, X., Liu, D., Li, M., Cao, C., Wan, D., Xi, B., Li, W., Tan, J., Wang, J., Wu, Z., et al. (2017). Prognostic and therapeutic value of disruptor of telomeric silencing-1-like (DOT1L) expression in patients with ovarian cancer. J. Hematol. Oncol. *10*, 29.

20. Lee, J.Y., and Kong, G. (2015). DOT1L: a new therapeutic target for aggressive breast cancer. Oncotarget *6*, 30451–30452.

21. Yao, Y., Chen, P., Diao, J., Cheng, G., Deng, L., Anglin, J.L., Prasad, B.V., and Song, Y. (2011). Selective inhibitors of histone methyltransferase DOT1L: design, synthesis, and crystallographic studies. J. Am. Chem. Soc. *133*, 16746–16749.

22. Quiñoà, E., and Crews, P. (1987). Phenolic constituents of Psammaplysilla. Tetrahedron Lett. *28*, 3229–3232.

23. Pereira, R., Benedetti, R., Pérez-Rodríguez, S., Nebbioso, A., García-Rodríguez, J., Carafa, V., Stuhldreier, M., Conte, M., Rodríguez-Barrios, F., Stunnenberg, H.G., et al. (2012). Indole-derived psammaplin A analogues as epigenetic modulators with multiple inhibitory activities. J. Med. Chem. *55*, 9467–9491.

24. Kim, H.J., Kim, T.H., Seo, W.S., Yoo, S.D., Kim, I.H., Joo, S.H., Shin, S., Park, E.S., Ma, E.S., and Shin, B.S. (2012). Pharmacokinetics and tissue distribution of psammaplin A, a novel anticancer agent, in mice. Arch. Pharm. Res. *35*, 1849–1854.

25. Hong, S., Shin, Y., Jung, M., Ha, M.W., Park, Y., Lee, Y.J., Shin, J., Oh, K.B., Lee, S.K., and Park, H.G. (2015). Efficient synthesis and biological activity of psammaplin A and its analogues as antitumor agents. Eur. J. Med. Chem. *96*, 218–230.

26. Steger, D.J., Lefterova, M.I., Ying, L., Stonestrom, A.J., Schupp, M., Zhuo, D., Vakoc, A.L., Kim, J.E., Chen, J., Lazar, M.A., et al. (2008). DOT1L/KMT4 recruitment and H3K79 methylation are ubiquitously coupled with gene transcription in mammalian cells. Mol. Cell. Biol. *28*, 2825–2839.

27. Anglin, J.L., and Song, Y. (2013). A medicinal chemistry perspective for targeting histone H3 lysine-79 methyltransferase DOT1L. J. Med. Chem. *56*, 8972–8983.

28. Scully, O.J., Bay, B.H., Yip, G., and Yu, Y. (2012). Breast cancer metastasis. Cancer Genomics Proteomics *9*, 311–320.

29. Poujade, F.A., Mannion, A., Brittain, N., Theodosi, A., Beeby, E., Leszczynska, K.B., Hammond, E.M., Greenman, J., Cawthorne, C., and Pires, I.M. (2018). WSB-1 regulates the metastatic potential of hormone receptor negative breast cancer. Br. J. Cancer *118*, 1229–1237.

30. Wen, S., Hou, Y., Fu, L., Xi, L., Yang, D., Zhao, M., Qin, Y., Sun, K., Teng, Y., and Liu, M. (2019). Cancer-associated fibroblast (CAF)-derived IL32 promotes breast cancer cell invasion and metastasis via integrin β3-p38 MAPK signalling. Cancer Lett. *442*, 320–332.

31. McGrath, J., and Trojer, P. (2015). Targeting histone lysine methylation in cancer. Pharmacol. Ther. *150*, 1–22.

32. Hirata, H., Hinoda, Y., Shahryari, V., Deng, G., Tanaka, Y., Tabatabai, Z.L., and Dahiya, R. (2014). Genistein downregulates onco-miR-1260b and upregulates sFRP1 and Smad4 via demethylation and histone modification in prostate cancer cells. Br. J. Cancer *110*, 1645–1654.

33. Zhang, X., Zheng, X., Yang, H., Yan, J., Fu, X., Wei, R., Xu, X., Zhang, Z., Yu, A., Zhou, K., et al. (2018). Piribedil disrupts the MLL1-WDR5 interaction and sensitizes MLL-rearranged acute myeloid leukemia (AML) to doxorubicin-induced apoptosis. Cancer Lett. *431*, 150–160.

34. Song, X., Gao, T., Wang, N., Feng, Q., You, X., Ye, T., Lei, Q., Zhu, Y., Xiong, M., Xia, Y., et al. (2016). Selective inhibition of EZH2 by ZLD1039 blocks H3K27 methylation and leads to potent anti-tumor activity in breast cancer. Sci. Rep. *6*, 20864.

35. Oktyabri, D., Ishimura, A., Tange, S., Terashima, M., and Suzuki, T. (2016). DOT1L histone methyltransferase regulates the expression of BCAT1 and is involved in sphere formation and cell migration of breast cancer cell lines. Biochimie *123*, 20–31.

36. Leconet, W., Chentouf, M., du Manoir, S., Chevalier, C., Sirvent, A., Aït-Arsa, I., Busson, M., Jarlier, M., Radosevic-Robin, N., Theillet, C., et al. (2017). Therapeutic activity of anti-AXL antibody against triple-negative breast cancer patient-derived xenografts and metastasis. Clin. Cancer Res. *23*, 2806–2816.

37. Liang, Y.K., Zeng, D., Xiao, Y.S., Wu, Y., Ouyang, Y.X., Chen, M., Li, Y.C., Lin, H.Y., Wei, X.L., Zhang, Y.Q., et al. (2017). MCAM/CD146 promotes tamoxifen resistance in breast cancer cells through induction of epithelial-mesenchymal transition, decreased ERα expression and AKT activation. Cancer Lett. *386*, 65–76.

38. Brabletz, T., Kalluri, R., Nieto, M.A., and Weinberg, R.A. (2018). EMT in cancer. Nat. Rev. Cancer *18*, 128–134.

39. Davis, F.M., Stewart, T.A., Thompson, E.W., and Monteith, G.R. (2014). Targeting EMT in cancer: opportunities for pharmacological intervention. Trends Pharmacol. Sci. *35*, 479–488.

40. Smith, P.K., Krohn, R.I., Hermanson, G.T., Mallia, A.K., Gartner, F.H., Provenzano, M.D., Fujimoto, E.K., Goeke, N.M., Olson, B.J., and Klenk, D.C. (1985). Measurement of protein using bicinchoninic acid. Anal. Biochem. *150*, 76–85.

41. Byun, W.S., Jin, M., Yu, J., Kim, W.K., Song, J., Chung, H.J., Jeong, L.S., and Lee, S.K. (2018). A novel selenonucleoside suppresses tumor growth by targeting Skp2 degradation in paclitaxel-resistant prostate cancer. Biochem. Pharmacol. *158*, 84–94.

42. Goldman, M., Craft, B., Hastie, M., Repecka, K., Kamath, A., McDade, F., Rogers, D., Brooks, A.N., Zhu, J., and Haussler, D. (2019). The UCSC Xena platform for public and private cancer genomics data visualization and interpretation. bioRxiv. https://doi.org/10.1101/326470.

43. Yook, J.I., Li, X.Y., Ota, I., Hu, C., Kim, H.S., Kim, N.H., Cha, S.Y., Ryu, J.K., Choi, Y.J., Kim, J., et al. (2006). A Wnt-Axin2-GSK3beta cascade regulates Snail1 activity in breast cancer cells. Nat. Cell Biol. *8*, 1398–1406.

44. Kim, W.K., Byun, W.S., Chung, H.J., Oh, J., Park, H.J., Choi, J.S., and Lee, S.K. (2018). Esculetin suppresses tumor growth and metastasis by targeting Axin2/E-cadherin axis in colorectal cancer. Biochem. Pharmacol. *152*, 71–83.

45. Vichai, V., and Kirtikara, K. (2006). Sulforhodamine B colorimetric assay for cytotoxicity screening. Nat. Protoc. *1*, 1112–1116.

46. Kwon, Y., Byun, W.S., Kim, B.Y., Song, M.C., Bae, M., Yoon, Y.J., Shin, J., Lee, S.K., and Oh, D.C. (2018). Depsidomycins B and C: new cyclic peptides from a ginseng farm soil-derived actinomycete. Molecules *23*, E1266.

47. Shin, D., Byun, W.S., Moon, K., Kwon, Y., Bae, M., Um, S., Lee, S.K., and Oh, D.C. (2018). Coculture of marine *Streptomyces* sp. with *Bacillus* sp. produces a new piperazic acid-bearing cyclic peptide. Front Chem. *6*, 498.

48. Kocatürk, B., and Versteeg, H.H. (2015). Orthotopic injection of breast cancer cells into the mammary fat pad of mice to study tumor growth. J. Vis. Exp. (96) https://doi.org/10.3791/51967..

49. Bradford, M.M. (1976). A rapid and sensitive method for the quantitation of microgram quantities of protein utilizing the principle of protein-dye binding. Anal. Biochem. *72*, 248–254.